Human Calf Muscle Metabolites Evaluated by ^{31}Phosphorous-Magnetic Resonance Spectroscopy as Biomarkers in Duchenne Muscular Dystrophy: Assessing the Reproducibility of Non-localized and Multivoxel Sequences

Hannah C. Rasmussen

University of Florida

Abstract

Background Duchenne Muscular Dystrophy (DMD) is an X-linked recessive disorder affecting males. It causes progressive muscle weakness, engendering early loss of ambulation and culminating in death. Many ongoing clinical trials show promise in finding a cure. Thus, there is a need for biomarkers which can detect drug efficacy and disease progression. ^{31}Phosphorus-magnetic resonance spectroscopy (^{31}P-MRS) has potential to be used as a sensitive, non-invasive biomarker of metabolic status in disease pathology. However, data concerning replicability of ^{31}P values is lacking. Further, studies which observe muscle-specific metabolites are scarce. In this study, a ^{31}P-MRS protocol was implemented to investigate metabolites in calves of control subjects using non-localized and multivoxel sequences. The objective was to determine whether ^{31}P spectra showed day-to-day reproducibility and which of the indices were the most sensitive across subjects.

Methods In this experimental study, ^{31}P-MRS spectra were collected from calf muscles of 5 unaffected control subjects (4 adults mean age 24.3±6.5 years,1 boy age 5 years) using non-localized and multivoxel sequences. A 3T MR scanner with ^{31}P circular surface coil (14cm diameter) was used to gather data at baseline and after 1 week. Spectra were graphed using jMRUI software as 7 peaks representing metabolite values. Metabolites measured included phosphocreatine (PCr), inorganic phosphate (P_i), ATP[(αATP+γATP+βATP)/3], and P_{tot}(P_i+PCr+αATP+γATP+βATP). The chemical shift between PCr and P_i was used to calculate pH. Variability was quantified by coefficient of variation (CV), and data compared using two-tailed t-tests.

Results ^{31}P data demonstrated acceptable day-to-day reproducibility in several indices of muscle metabolism in both non-localized and multivoxel scans. ATP/P_{tot}, PCr/P_{tot}, and pH showed the best day-to-day consistency in adult subjects and the child (CV<10%). Reproducibility in metabolite ratios was also noted across subjects. Values influenced by ßATP

tended to associate with increased variability. For many values, reproducibility of multivoxel scans was similar ($p>0.05$) to reproducibility of non-localized.

Conclusion These findings characterized ^{31}P-MRS indices in the calf by indicating that metabolite values, most notably those of ATP/P_{tot}, PCr/P_{tot}, and pH have potential to be sensitive and reproducible, both in multivoxel and non-localized sequences.

Public Health and/or Health Professions Relevance ^{31}P-MRS has the potential to qualify as a sensitive and non-invasive biomarker of DMD pathology.

Funding NIH NIAMS: R01AR070101

Student Role Over the course of this study, Hannah Rasmussen took part in subject recruitment, data collection, image processing, and quantitative analysis.

Human Calf Muscle Metabolites Evaluated by ^{31}Phosphorous-Magnetic Resonance Spectroscopy as Biomarkers in Duchenne Muscular Dystrophy: Assessing the Reproducibility of Non-localized and Multivoxel Sequences

Literature Review

Duchenne Muscular Dystrophy (DMD) is a severe and progressive muscle wasting disease which impacts 1 in every 3,500-6,000 boys (Mendell et al., 2012). DMD is the consequence of an X-linked recessive mutation in the gene that codes for dystrophin such that the protein is either defective or absent (Vohra et al., 2015). As dystrophin acts to link the myofibril cytoskeleton to the extracellular matrix, dystrophic muscle is vulnerable to damage from mechanical stress. When satellite cells cannot maintain repair, rapidly damaged muscle is replaced by fatty and fibrotic tissue (Latroche et al., 2015). Myocytic degeneration, regeneration and replacement are concurrent with inflammation, abnormalities in ionic homeostasis and energy metabolism, and decreased regenerative capabilities (Reyngoudt, Turk, & Carlier, 2018). Progressive fatty infiltration and muscle weakness engender an early loss of ambulation, around the age of 8-12 years, and a reduced life expectancy due to cardiopulmonary complications, around the age of 20-30 years (Deconinck & Dan, 2007; Humbertclaude et al., 2012).

Although there is no cure for DMD, upcoming therapeutic interventions such as exon skipping, utrophin upregulation, and stop codon suppression compounds show promise in compensating for the defective dystrophin-coding gene (Willcocks et al., 2016). Corticosteroids, which aim to mitigate inflammation and thereby improve quality of life, are considered to be the current standard of care (Reinig, Mirzaei, & Berlau, 2017). Treatment is most beneficial when begun prior to severe muscle wasting, around the age of 5, to delay the onset of cardiac, orthopedic, and respiratory dysfunction (Forbes et al., 2014). Therefore, there is a need for sensitive, reliable biomarkers which detect disease progression even in young boys, and which are responsive to treatment in clinical trials.

Functional tests are the current canon of disease progression, preferred by many over invasive measures such as muscle biopsies (Willcocks et al., 2016). However, the FDA-approved 6 Minute Walk Test has been criticized for having narrow inclusion criteria, for only showing disease progression in boys over the age of 7 and for having low inter-operator reproducibility (Forbes et al., 2014). Recent studies have shown magnetic resonance imaging (MRI) and spectroscopy (MRS) to be sensitive and non-invasive measures of inflammation and fat infiltration in muscles of young boys with DMD (Willcocks et al., 2016). These indices have displayed reproducibility when measured across multiple institutions, and over the span of several days (Triplett et al., 2013). Furthermore, these MRI and MRS quantifications have been used to detect the positive impact of corticosteroids on dystrophic muscle, validating their usefulness as indices for other treatments (Arpan et al., 2014; Wary et al., 2015). However, many concur that there is still a need for a replicable biomarker of DMD in young boys which is both able to characterize pathology in the muscle itself and able to discriminate disease status in spite of corticosteroid use (Hooijmans et al., 2017).

^{31}Phosphorous-magnetic resonance spectroscopy (^{31}P-MRS) has been used to identify numerous aberrations in phosphate metabolite ratios in DMD research over the years. These ratios of phosphate energetics and membrane metabolites reflect disease anomalies at a cellular level (Wary et al., 2015). ^{31}P-MRS principally observes spectra from myocytes, as bioenergetic values are almost undetectable in fat (Hooijman et al., 2017). A recent study by Wary et al. (2015) showed that metabolic indices were all exaggerated in more affected boys with DMD, and were already altered relative to normal in younger boys with DMD. Additionally, increased phosphodiester (PDE) ratios have been shown to reflect pathologic changes in dystrophic muscle as early as 5 years of age, independent of fatty infiltration (Hooijmans et al., 2017; Reyngoudt et al., 2018). Furthermore, the sensitivity of ^{31}P indices to therapeutic intervention has been assessed using Golden Retriever Muscular Dystrophy (GRMD) canines,

the animal model most comparable to human DMD. These studies have reported on improved phosphate metabolism values in the forelimbs of GRMD canines following exon skipping therapy (Le Guiner et al., 2014; Le Guiner et al., 2017; Thibaud et al., 2012). Banerjee et al. (2010) showed that ^{31}P-MRS measures were sensitive enough to detect short-term changes in the calves of boys with DMD following oral creatine supplementation, including in young boys under the age of 7. These results infer the use of ^{31}P-MRS as a valuable indicator with the potential to detect changes in metabolic status following therapeutic intervention, even from a young age.

The structure of clinical trials renders gathering ^{31}P-MRS data across several subjects and over time necessary for making accurate comparisons. However, confounding variables across individuals and over days may reduce the reliability of MR measures. These confounds include inter-operator variability, and differences in subject positioning and sequence configurations. One procedure which acts to reduce the impact of these variables on data is the utilization of a phantom. A phantom is a canon which can be tested regularly to detect deviations in scanner performance, and to correct data to make valid comparisons. The inorganic phosphate (P_i) phantom was designed as part of this project to resemble P_i stored in the skeletal muscle of the human leg. Human controls are also utilized in MR data acquisition for many purposes. The first is in detecting variability in ^{31}P data both day-to-day and across subjects. Metabolic indices which vary minimally across scans are more reproducible measures. Human controls are also useful for developing standardized methods for positioning subjects and for selecting muscles of interest (Forbes et al., 2013). Finally, ^{31}P-MRS spectra collected from the skeletal muscle of human controls can be compared to spectra from boys with DMD, and can be held as a standard against which to be measured in future trials.

In this study, a ^{31}P-MRS protocol was implemented to investigate metabolite values in a ^{31}P Lego Phantom and in the calves of unaffected human control subjects. The aims of this

study were as follows: 1) to determine whether the ^{31}P Lego Phantom showed acceptable reproducibility over several weeks; 2) to assess whether non-localized ^{31}P-MRS spectra collected simultaneously from all calf muscles of human control subjects differed across days scanned; 3) to observe whether multivoxel ^{31}P-MRS spectra collected from certain calf muscles of controls were reproducible, and, further, to determine whether any significant differences existed among selected calf muscles; 4) to evaluate which of the metabolite ratios collected from both the spatially localized and un-localized scans were the most sensitive across subjects and had the highest day-to-day reproducibility; 5) to consider whether significant differences existed between the reproducibility of data gathered from the multivoxel and non-localized ^{31}P-MRS sequences.

Methods

This experimental study was approved by the institutional review board at the University of Florida, and was conducted in compliance with the Health Insurance Portability and Accountability Act. Informed written consent was obtained from the subject or guardian before study participation.

Phantom Studies

The P_i Lego Phantom was created with a two-compartment coaxial geometry. The inner compartment contained potassium monophosphate, while the outer compartment contained potassium diphosphate, both diluted to simulate P_i values in the skeletal muscle of the human calf. One phantom was created and scanned seven times over the course of 7 months to detect day-to-day variability in data. Non-localized and multivoxel (4 × 4 voxel and 8 × 8 voxel) sequences were collected and analyzed. P_i monobasic and P_i dibasic were each represented by a Lorentzian curve with only a single peak. If more than one peak was present, the data was

excluded from analysis. Data was acquired and quantified using standardized protocols which paralleled those used for human controls (see below).

Participants

Four unaffected adult subjects (mean age, 24.3 ± 6.5 years [standard deviation]; range, 21–35 years) and one young boy (5 years of age) were recruited to participate in this study**.** Participants were asked to avoid physical activity beyond their normal level for three days prior to each scan**.** All controls completed measurements both at baseline and 1-week follow-up.

^{31}P-MRS Data Acquisition

All spectra were collected by a Philips 3T whole-body MRI scanner using a circular phosphorous surface coil (diameter=14cm). Standardized operating procedures were implemented across scans including subject positioning and routine scan protocol. The imaging protocol contained a 2D-Chemical Shift Imaging (2D-CSI) data set to assess energy metabolism. Total time in the scanner, including time for set-up, did not exceed 40 minutes per subject. During the scan, patients lay supine, feet-first, their calf centered in the bore of the magnet and elevated over rice bags. The widest portion of the subjects' right calf was centered over the phosphorous surface coil and secured by foam padding to minimize movement.

Proper positioning was assessed using a T1- weighted survey scan with 2.5mm slice thickness (1.34min, TR=7.2ms, TE=3.5ms) and a T2- weighted spin echo sequence with 7mm slice thickness (slices=4, NSA=1, TR=3,000ms, TE=20ms, n=16, 20-320ms, each separated by 20ms).

Non-localized data. Un-localized MR sequences enable analysis of metabolite ratios gathered simultaneously from all skeletal muscles of the calf. Non-localized data was collected from the right calf of each subject at a repetition time (TR) of 5,000ms and an echo time (TE) of

0.10ms. The number of signal averages (NSA) collected was 4, totaling a 20-second acquisition time for each patient. Non-localized data was graphed as 7 Lorentzian resonances, shown in Figure 1.

Multivoxel data. Spatially localized sequences allow for the collection of muscle-specific metabolite ratios. Multivoxel data was collected from the right calf, and voxels from the soleus (Sol) and medial gastrocnemius (MG) were analyzed as free induction decays as shown in Figure 2. For these scans, the TR was 3000ms, the TE was 0.31ms, and the NSA collected was 8. For all except for the 5×5 sequence, spatial zero-filling was set to 4 for an increased matrix size.

The first scan consisted of a 4 by 4 voxel matrix (zero-filled to 8 × 8 voxel matrix, each voxel was 35mm × 35mm with 60mm slice thickness) with a total acquisition time of 6.4 minutes. The four adult control subjects each completed a 4 × 4 multivoxel scan both at baseline and 1-week follow-up. Of note, the young control underwent a repeated 5 × 5 voxel scan (each voxel was 20mm × 20mm with 60mm slice thickness) with a total acquisition time of 7.4 minutes.

The second scan consisted of an 8 × 8 voxel matrix (zero-filled to 16 × 16 voxel matrix, each voxel was 17.5mm × 17.5mm with 30mm slice thickness) for a total acquisition time of 25.6 minutes. Localized 8 × 8 scans were collected on one acquisition day each for volunteers 1, 3 and 4. The tibialis anterior (TA) was analyzed in addition to the Sol and MG during these scans.

Spectra collected by the Philips 3T were converted to digital imaging and communications in medicine (DICOM) files and analyzed using ImageJ (NIH) software. The spin echo image taken at 20ms TE was overlaid with spectra using jMRUI, and muscles of interest were carefully selected by standardizing the number and position of voxels chosen from the

slices. Voxels with at least 75% of their surface area overlaying the muscle of interest were considered acceptable, while voxels overlapping multiple muscles or voxels containing primarily fat or bone were not used for analysis (Figure 3).

^{31}P-MRS Data Analysis

Data analysis procedures were standardized across scans including the selection of key voxels, the use of prior knowledge, the setting of PCr as the zero-reference, zero-filling, apodizing, and phasing. Metabolite resonances were evaluated using jMRUI (http://www.jmrui.eu/welcome-to-the-new-mrui-website), and the total signal was fitted with AMARES, a non-linear least-squares quantitation algorithm. Starting values and prior knowledge were created and used to tighten constraints for more accurate quantitation. Line widths were kept under 40Hz.

Metabolic values were calculated by fitting in the time domain for seven Lorentzian ^{31}P spectral peaks (Figure 4). Phosphorous peaks corresponded to phosphomonoester (PME), inorganic phosphate (P_i), phosphodiester (PDE), phosphocreatine (PCr), γ-ATP, α-ATP, and β-ATP, respectively. Shimming was only considered satisfactory if the PCr full line width at half maximum (FWHM) was less than 100Hz. Resonances which were not visible due to low signal-to-noise ratio were excluded from analysis. For some of the multivoxel scans, the signal-to-noise ratio of PDE, PME and β-ATP was not acceptable for accurate quantitation.

Collected values were then analyzed as 15 ratios of interest (ATP/P_{tot}, PCr/ β-ATP, PCr/ γ-ATP, PCr/ATP, PCr/P_{tot}, PDE/β-ATP, PDE/ γ-ATP, PDE/ATP, PDE/P_{tot}, P_i/ β-ATP, P_i/ γ-ATP, P_i/ATP, P_i/P_{tot}, P_i/PCr, and PME/P_{tot}). ATP was defined as [(α-ATP+ γ-ATP+ β-ATP)/3], and P_{tot} was defined as (P_i+PCr+ α-ATP+ γ-ATP+ β-ATP). The pH of each subject's calf was determined by the chemical shift between PCr and P_i resonances according to the equation $pH = 6.75 + \log[(3.27 - S)/(S - 5.69)]$.

Statistical Analysis

Variability in metabolite ratios across scans was computed using standard deviation (σ) and coefficient of variation (CV). CV was calculated individually for each subject by dividing the standard deviation of the repeated measures by the mean of the repeated measures, and multiplying the result by 100%. The mean of the CV of all five subjects was then calculated and used to infer variability across participants and days scanned. A CV<10% was necessary for measures to be considered reproducible. The CV was calculated in all phantom scans, the non-localized human scans and the multivoxel human scans, for each ratio of interest and for pH.

Correlation between all other key data sets was calculated using two-tailed Student's T-tests. Comparisons were made between the reproducibility of un-localized and multivoxel data (4×4 voxel) by conducting a two-tailed t-test, each array being composed of the CV of the five subjects. These t-tests were conducted for each of the metabolic indices, and the mean of the non-localized data was compared to the mean of the Sol and the MG separately. T-tests were also used to compare metabolic indices from the scan at baseline and the scan at follow-up for each of the sequences to analyze whether any systematic differences occurred across days scanned. Finally, a two-tailed t-test was performed for each of the ratios and pH to determine whether the ^{31}P values collected from the MG and Sol were similarly reproducible. P-values>0.05 were considered necessary in determining that no significant differences existed between data sets of interest.

Results

The P_i Lego Phantom was scanned seven times over the course of 7 months. Of the 36 resonances collected, 34 met criteria for analysis. ^{31}P-MRS spectra were collected from the calf muscles of five unaffected controls both at baseline and after 1 week for a total of 10 scans. All 90 spectra collected from un-localized scans at baseline and follow-up met quality control

criteria. For the multivoxel data, 199 out of 203 resonances collected from baseline and follow-up met quality control criteria. CV<10% was considered a noteworthy value in assessing for replicability and sensitivity of metabolic indices. A p-value>0.05 was necessary to establish that no significant differences existed between two data sets.

Phantom Studies

In the non-localized phantom scans, P_i monobasic/ P_i dibasic had a CV of 13.9% for the six scans which met criteria for analysis. Interestingly, the amplitude ratios of scans 1, 2 and 5 were identical at 1.72 each. As seen in figure 5, scan 3 was an outlier in that it had a higher amplitude of 3.40, owing to an increased P_i dibasic value. The finding that the CV of the non-localized scans was not consistently low suggests that this measure may be sensitive to potential variations in set-up or acquisition from day-to-day, such as small changes in coil position, shimming, or signal-to-noise ratio.

In the way of the seven 4×4 multivoxel phantom scans, a CV of 9.14% was observed for the outer compartment (σ=0.245), and a CV of 18.20% was observed for the inner compartment (σ =0.0992). CV is more affected by outliers when analyzing quantitative variables less than 1, as was the case when analyzing the amplitude ratio of the phantom inner compartment. Therefore, the standard deviation is also important to consider in determining how spectra varied across scans. In this case, the low inner compartment CV, as well as the low outer compartment σ, were sufficient to suggest that there may have been minimal variation across 4×4 scans (Figure 6). The 8×8 multivoxel phantom scans had a CV of 29.3% for the outer compartment amplitude ratio (σ=1.33), and a CV of 11.9% for the inner compartment amplitude ratio (σ =0.036). The variation in the outer compartment was likely influenced by an increased P_i monobasic amplitude on scan 5, as the 8×8 sequence was only performed during three scans.

Non-Localized Human Control Studies

For all 15 metabolite ratios collected as well as for pH, $p>0.05$ for the t-test which was conducted to compare day 1 scans to day 2 scans for volunteers 1-5. This suggests that there were likely no systematic differences between spectra collected at baseline and 1-week follow-up. Thus, non-localized sequences may have displayed high day-to-day replicability in adult controls, as well as in the young child.

Multivoxel Human Control Studies

Data also showed that it was probable that no systematic differences existed between the repeated ^{31}P-MRS scans in the Sol, as was evidenced by $p>0.05$ for all metabolic indices evaluated in the 4×4 scans. In the MG, all bioenergetic values except for those of PDE were associated with $p>0.05$ when comparing the scan at baseline to the follow-up scan. Ratios of PDE (PDE/ β-ATP, PDE/ γ-ATP, PDE/ATP, and PDE/P_{tot}) rendered p-values<0.05. Therefore, some day-to-day variability in PDE may have existed among the 4×4 MG scans. 15 metabolic indices and pH were also compared between the Sol and the MG via two-tailed t-test. All 16 of these data sets were characterized by a $p>0.05$, suggesting that spectra gathered from the two muscles of interest have the potential to be similarly reproducible.

Day-to-day Reproducibility in Human Controls

To determine day-to-day replicability and variation across subjects, the CV was calculated individually for each repeated measure. Then, the CV of all 5 volunteers were averaged for each ratio and compared. Regarding non-localized data, ATP/P_{tot} (CV=5.93±3.56%), PCr/ γ-ATP (CV=9.64±5.85%), PCr/P_{tot} (CV=6.07±3.42%), and pH (CV=0.28±0.238%) had CV which were sufficiently low to associate these values with minimal day-to-day variability and high sensitivity across subjects. Values influenced by β-ATP tended to be associated with increased CV (23.4±13%<CV<27.5±15%). Additionally, PDE and PME had

miniscule amplitude ratios (<1) such that they were associated with a relatively large CV (10.4±6.7%<CV<22.7±25%) (Table 1).

In the way of 4×4 multi-voxel data, the Sol also had many indices associated with a significantly low CV. Owing to their CV<10%, ATP/P_{tot} (CV=7.35±5.68%), PCr/P_{tot} (CV=8.00±6.26%) and pH (CV=0.22±0.110%) of the Sol may have reduced day-to-day variability (Table 2). For MG values, only pH had an adequately low CV (CV=0.50±0.710%) (Table 3). For both the MG and the Sol, β-ATP was correlated with a higher CV (Sol: 21.3±16.8%<CV<43.4± 24.9%; MG: 36.8±26.3% <CV<64.0±7.23%). PDE and PME had small amplitude ratios (<1) which caused their CV to be increased compared to other metabolic indices (Sol: 29.5±28%<CV<43.4± 24.9%; MG: 56.7±49.8% <CV<64.0±7.23%).

Reproducibility was measured in the 8×8 multivoxel scans by calculating the CV of the 3 single scans which were performed. PCr/P_{tot} (2.11±1.21%<CV<9.23±5.37%) and pH (0.16±1.15%<CV<3.76±26.5%) had a sufficiently minimal CV for the Sol, MG and TA alike (Table 4).

Notably, PCr/P_{tot} and pH each had a significantly low CV across the majority of ^{31}P-MRS sequences conducted in this study. Thus, these two metabolic indices have the potential to be associated with minimal day-to-day variability and increased sensitivity across subjects, both in the adults and in the young child.

Comparing Non-Localized and Multivoxel Data in Human Controls

For all 15 bioenergetic ratios and pH, t-tests were conducted to compare the reproducibility of non-localized data to the reproducibility of 4×4 data from both the Sol and the MG. For all t-tests comparing non-localized data to the Sol, $p>0.05$. A p-value>0.05 implies that no systematic differences existed between the reproducibility of the un-localized scan and the scan localized to the Sol. Six of the 16 t-tests conducted to compare the reproducibility of non-

localized values to those of the MG were associated with p-values<0.05 (PDE/β-ATP, PDE/γ-ATP, PDE/ATP, PDE/P_{tot}, P_i/ATP, and P_i/P_{tot}). Therefore, un-localized PDE and P_i values were different than localized PDE and P_i values in the MG. These findings may indicate that multivoxel scans are sensitive enough to detect subtle changes in PDE and P_i values in specific skeletal muscles, supporting the value in conducting localized measures.

Discussion

This experimental study evaluated the sensitivity and day-to-day reproducibility of metabolites quantified using non-localized and multivoxel ^{31}P-MRS sequences. A standardized MR protocol using ^{31}Phosphorus 2D-CSI was implemented in both a coaxial P_i Lego Phantom and the calf muscles of 5 unaffected human control subjects (4 adults, age range 21-35; 1 boy age 5 years). The P_i phantom was scanned 7 times over 7 months, and control subjects were scanned at baseline and 1-week follow-up. The time domain of the ^{31}P resonances collected from the scan was fitted to quantify myocytic metabolites. These amplitudes were then presented as ratios and compared to observe for day-to-day variability and accuracy.

Our primary findings were that: 1) the P_i phantom accurately detected variability between scans in both non-localized and multivoxel ^{31}P-MRS sequences; 2) there were no systematic differences between indices quantified by repeated non-localized scans (p>0.05); 3) most values collected by multivoxel 4×4 scans displayed minimal variability (p>0.05) across days except for metabolic ratios involving PDE in the MG. Further, metabolic indices in the MG and Sol quantified by 4×4 multivoxel sequences were similarly reproducible (p>0.05); 4) ATP/$P_{tot,}$ PCr/P_{tot} and pH were found to be the most highly reproducible indices across days scanned, and the most sensitive across subjects (CV<10%). Moreover, bioenergetic ratios influenced by β-ATP tended to have lower sensitivity and repeatability (CV>10%). These findings were true for the 4 adult controls and the young child alike; 5) spatially resolved human scans have day-to-day reproducibility that is comparable to the reproducibility of non-localized scans. This was true

for all bioenergetic ratios except for those involving PDE and some of those involving P_i in the MG.

Upcoming therapeutic interventions with the potential to alter the course of DMD would benefit from sensitive, non-invasive biomarkers of disease progression. Recent studies have observed ^{31}P-MRS values of metabolic function in DMD patients which differ significantly from those in controls (Wary et al., 2015). DMD is quantified by ^{31}P-MRS as a graph with archetypal metabolite anomalies, including: a double P_i peak (cytosolic and pooled inorganic phosphate); increased total P_i, PME and PDE; and decreased PCr (Wary, Naulet, Thibaud, Monnet, Blot, & Carlier, 2012). Many have speculated that dystrophin deficiency in DMD is the origin of these abnormal indices, as dystrophin is implicated in the regulation of calcium ion concentrations. Because Ca^{2+} coordinates enzyme function, dystrophin-deficient muscle may be susceptible to alterations in energy metabolism (Sharma et al., 2003).

In establishing how ^{31}P indices in boys with DMD differ from those in unaffected controls, studies have specifically analyzed how ^{31}P-MRS ratios differ with age, inflammation and fat infiltration in both animal and human models of the disease (Latroche et al., 2015; Sharma et al., 2003; Wary et al., 2012). Although these aberrations in DMD bioenergetics have been well-established, they are poorly understood. For instance, researchers have delineated that phosphodiester (PDE) values are increased in the skeletal muscle of subjects with DMD compared to controls (Reyngoudt et al., 2018). However, data regarding the exact origin of these increased products of membrane degradation as well as their evolution with disease progression has yet to be established (Banerjee et al., 2010; Hooijmans et al., 2017). The study at hand was useful in better characterizing metabolite values in the calf by detecting which were the most sensitive and replicable, and by determining how bioenergetic ratios differ among muscles, using both a P_i phantom and unaffected human control subjects.

Replicability and Accuracy of ^{31}P Indices in Human Controls

While a growing body of evidence has shown how bioenergetic values differ in boys with DMD compared to unaffected boys, not much has been done in the way of evaluating the day-to-day variability of metabolic indices as measured by ^{31}P-MRS sequences. It is beneficial to better characterize these values by establishing which of the phosphorous ratios is the most sensitive and repeatable. By so doing, we can expand upon previous research and further evaluate the usefulness of ^{31}P-MRS as an efficacious biomarker of DMD pathology.

Replicability was evaluated in the calves of five human controls by observing how seven metabolic resonances vary at baseline and after one week. The presentation of the seven peaks of interest in human controls was relatively consistent. ATP was characterized by a β-ATP peak downstream of the two neighboring γ-ATP and α-ATP peaks, α-ATP often nearly overlapping PCr. PCr was characterized by a large, centrally-located peak. Quantification of ATP/P_{tot} and PCr/P_{tot} proved to be highly reproducible and sensitive with a mean within-subject CV<10% in both the non-localized and 4×4 Sol scans. This was true for all four adult subjects, as well as for the young child. These ratios were not as reproducible in the 4×4 MG scan, (CV>10%) likely because the MG had a lower signal-to-noise ratio than the Sol since it had a greater offset from the center of the coil (Figure 2). Notably, PCr/Ptot showed high reproducibility for all three selected muscles in the 8×8 multivoxel scans as well, although these sequences were conducted only once each on three subjects. β-ATP was shown to be a less sensitive biomarker compared to the other metabolites as revealed by its high CV across all sequences and in all subjects. We hypothesized that this was because its resonance frequency was further from the zero reference (center frequency), and because it was often associated with a lower signal-to-noise ratio than were other peaks.

ATP and PCr are both high-energy phosphate stores essential for muscle contraction. PCr stored in the muscle donates its phosphate group to ADP to generate ATP, and the rate of ATP production and utilization defines a muscle's energetic state. A decreased PCr peak may

be indicative of a pathologic status, such as in DMD (Banerjee et al., 2010). Reduced PCr may be associated with membrane instability, which leads to enzyme dysregulation and an inability of the myocyte to uptake glucose for glycolysis (Sharma et al., 2003). ATP resonances do not vary significantly in DMD pathology (Raymond et al., 1982). Because PCr spectra were shown to be both sensitive and replicable, even in the young subject, this high-energy metabolite may be used to characterize DMD pathology in future trials.

The PDE and PME peaks were both slight in all subjects and across both non-localized and multivoxel scans. Because their amplitude ratios were so small, they were associated with a relatively large CV. Further, the PDE peak did not meet criteria for analysis in the 4×4 scan of the MG for volunteer 3, and PME did not meet criteria in the 4×4 scan of the Sol for volunteer 5. These excluded resonances may have also impacted the magnitude of the CV.

The PME peak is composed primarily of glucose-6-phosphate, an intermediate molecule in the breakdown of glucose during glycolysis. Some suggest that an increased PME peak is characteristic of dystrophic muscle, which is easily fatigued and lacks normal levels of lactic acid production due to an inability to use glucose efficiently (Wehling-Henricks, Oltmann, Rinaldi, Myung, & Tidall, 2009). PDE represents catabolized components of the lipid bilayer. It has been suggested that high PDE amplitudes may correlate to a higher rate of cell wall turnover, reflecting a diseased state (Banerjee et al., 2010; Wary et al., 2012). A recent study by Hooijman et al. (2017) using a 7T MR system revealed that PDE was highly reproducible with a mean within-subject CV of 4.3% in datasets with high signal-to-noise ratio, and 5.7% in datasets with low signal-to-noise ratio, in four adult controls. This study also found that in DMD, PDE was elevated independent of fat fraction, even in boys as young as 5 years old. Thus, although PDE was not found to be highly reliable at 3T, this resonance has the potential to be sensitive to disease pathology, even from a young age.

The pH of each subject's calf was determined by the distance between PCr and P_i. In this study, pH had the lowest CV of all metabolic indices and across all sequences, both in the adult subjects and the young child. Alkaline pH is one of the most consistent indicators of DMD pathology across age, muscle of interest and severity, as well as one of our most sensitive and reproducible biomarkers (Hooijman et al., 2017). It has been suggested that a more basic P_i resonance would be reflective of oxidative phosphorylation dysregulation or leaky membranes which would lead to energy wasting (Reyngoudt et al., 2018; Wary et al., 2012).

By establishing which of the myocytic metabolites quantified by ^{31}P-MRS are the most sensitive and repeatable, we can expand upon and verify previous research. For instance, Banerjee et al. (2010) found that PCr/P_i and PCr/β-ATP showed the most significant difference between boys with DMD and unaffected human controls. Findings from the research at hand suggest that follow-up studies should focus more on the PCr/P_i metabolic ratio, as it is the more sensitive ratio.

Multivoxel Studies of ^{31}P Indices in Human Controls

There is also a shortage of research which analyzes metabolite ratios via spatially localized sequences. The collection of muscle-specific ^{31}P indices is necessary because muscles in patients with DMD become affected at different stages and progress at different rates within the disease process (Hooijmans et al., 2017). Typically, type II fast twitch muscle fibers such as the MG are more affected by DMD (Wary et al., 2012).

Recent DMD research has benefitted greatly from observing proton transverse relaxation time (T_2) among individual muscles. Researchers found that in DMD, the MG and Sol had an increased T_2, while the TA (medially) was relatively spared, even in boys from a young age. Further, muscle-specific T_2 values have been shown to be more sensitive than are mean T_2 measures. Water T_2 has also been implicated as a biomarker capable of detecting subtle

changes among specific muscles in disease pathology, even from a young age (Arpan et al., 2013). Overall, these MR studies support the importance of studying disease progression in individual muscles.

A recent study by Hooijmans et. al (2017), assessed muscle-specific ^{31}P values in the calves of boys with DMD compared to age-matched controls. The study found that in DMD, P_i/PCr was increased in all muscles at baseline, and increased only in the Sol at 24 months follow-up. It was also observed that pH was more alkaline in the Sol, MG and TA of boys with DMD at all time points. Many metabolite ratios were found to be impacted differently among muscles at varying time points in DMD pathology. These findings indicate that ^{31}P values may detect differences in muscle tissue status throughout the disease process.

The study at hand has also helped to establish the use of multivoxel sequences at 3T as efficacious biomarkers of DMD progression by showing that, overall, they have reproducibility which is similar to that of non-localized scans. One disadvantage to the use of multivoxel sequences is that they result in added time in the MR scanner. While the non-localized scan takes only 20 seconds, the 4×4 scan takes 7 minutes, and the 8×8 scan takes 26 minutes. Thus, these spatially resolved scans may be more susceptible to effects from movement and loss of participant attention. Nonetheless, there is potential for multivoxel measures of bioenergetic indices to be specific, and to have the ability to detect subtle changes in varying muscles of boys with DMD even from a young age.

This study observed the replicability of phosphorous metabolites in the calves of human control subjects using both localized and non-localized ^{31}P-MRS sequences. Results revealed that ATP/P_{tot}, PCr/P_{tot} and pH showed the greatest day-to-day reproducibility of the metabolite ratios examined. Further, spectra collected from the non-localized scan and the multivoxel scan were shown to be similarly reproducible. However, because some spectra failed to meet quality control criteria, they were excluded from analysis. This may have biased some of the CV and p-

values of the 16 metabolic indices. Additionally, this study was limited by its small sample size which consisted primarily of adult subjects. Future studies should verify whether this adult population is fully translatable to a population of young boys. The use of larger sample sizes and young controls may help to better elucidate whether multivoxel and non-localized ^{31}P-MRS sequences may serve as sensitive, replicable biomarkers with the potential to detect drug efficacy and disease progression in young boys with DMD.

References

Arpan, I., Forbes, S. C., Lott, D. J., Senesac, C. R., Daniels, M. J., Triplett, W. T., & ... Vandenborne, K. (2013). T2 mapping provides multiple approaches for the characterization of muscle involvement in neuromuscular diseases: a cross-sectional study of lower leg muscles in 5-15-year-old boys with Duchenne muscular dystrophy. *NMR In Biomedicine*, 26(3), 320. doi:10.1002/nbm.2851

Arpan, I., Willcocks, R. J., Forbes, S. C., Finkel, R. S., Lott, D. J., Rooney, W. D., . . . Vandenborne, K. (2014). Examination of effects of corticosteroids on skeletal muscles of boys with DMD using MRI and MRS. *Neurology,* 83(11), 974-980. doi:10.1212/WNL.0000000000000775

Banerjee, B., Sharma, U., Balasubramanian, K., Kalaivani, M., Kalra, V., & Jagannathan, N. R. (2010). Effect of creatine monohydrate in improving cellular energetics and muscle strength in ambulatory Duchenne muscular dystrophy patients: a randomized, placebo-controlled 31P MRS study. *Magnetic Resonance Imaging* (0730725X), 28(5), 698-707. doi:10.1016/j.mri.2010.03.008

Deconinck, N., & Dan, B. (2007). Pathophysiology of Duchenne Muscular Dystrophy: Current Hypotheses. Pediatric Neurology, (1), 1.

Forbes, S., Willcocks, R., Triplett, W., Rooney, W., Lott, D., Wang, D., . . . Vandenborne, K. (2014). Magnetic resonance imaging and spectroscopy assessment of lower extremity skeletal muscles in boys with duchenne muscular dystrophy: A multicenter cross sectional study. *Plos One*, 9(9), e106435. doi:10.1371/journal.pone.0106435

Hooijmans, M. T., Doorenweerd, N., Baligand, C., Verschuuren, J. M., Ronen, I., Niks, E. H., & ... Kan, H. E. (2017). Spatially localized phosphorous metabolism of skeletal muscle in

Duchenne muscular dystrophy patients: 24–month follow-up. *Plos ONE*, 12(8), 1-15. doi:10.1371/journal.pone.0182086

Humbertclaude, V., Hamroun, D., Bezzou, K., Bérard, C., Boespflug-Tanguy, O., Bommelaer, C., & ... Tuffery-Giraud, S. (2012). Original article: Motor and respiratory heterogeneity in Duchenne patients: Implication for clinical trials. *European Journal Of Paediatric Neurology*, 16149-160. doi:10.1016/j.ejpn.2011.07.001

Latroche, C., Matot, B., Martins-Bach, A., Briand, D., Chazaud, B., Wary, C., . . . Jouvion, G. (2015). Structural and functional alterations of skeletal muscle microvasculature in dystrophin-deficient mdx mice. *American Journal of Pathology*, 185(9), 2482-2494. doi:10.1016/j.ajpath.2015.05.009

Le Guiner, C., Montus, M., Servais, L., Cherel, Y., Francois, V., Thibaud, J., & ... Voit, T. (2014). Original Article: Forelimb Treatment in a Large Cohort of Dystrophic Dogs Supports Delivery of a Recombinant AAV for Exon Skipping in Duchenne Patients. *Molecular Therapy,* 221923-1935. doi:10.1038/mt.2014.151

Le Guiner, C., Servais, L., Montus, M., Larcher, T., Fraysse, B., Moullec, S., & ... Dickson, G. (2017). Long-term microdystrophin gene therapy is effective in a canine model of Duchenne muscular dystrophy. *Nature Communications*, 816105. doi:10.1038/ncomms16105

Mendell, J. R., Shilling, C., Leslie, N. D., Flanigan, K. M., al-Dahhak, R., Gastier-Foster, J., & ... Weiss, R. B. (2012). Evidence-based path to newborn screening for Duchenne muscular dystrophy. *Annals Of Neurology*, 71(3), 304-313. doi:10.1002/ana.23528

Raymond J., N., Peter J., B., Lawrence, C., David G., G., Peter, S., Doris, T., & George K., R. (1982). Nuclear Magnetic Resonance Studies Of Forearm Muscle In Duchenne Dystrophy. *British Medical Journal* (Clinical Research Edition), (6322), 1072.

Reinig, A. M., Mirzaei, S., & Berlau, D. J. (2017). Advances in the Treatment of Duchenne Muscular Dystrophy: New and Emerging Pharmacotherapies. Pharmacotherapy: The *Journal Of Human Pharmacology And Drug Therapy*, (4), 492. doi:10.1002/phar.1909

Reyngoudt, H., Turk, S., & Carlier, P. G. (2018). 1H NMRS of carnosine combined with 31P NMRS to better characterize skeletal muscle pH dysregulation in Duchenne muscular dystrophy. *NMR In Biomedicine*, (1), doi:10.1002/nbm.3839

Sharma, U., Atri, S., Sharma, M., Sarkar, C., & Jagannathan, N. (2003). Regular article: Skeletal muscle metabolism in Duchenne muscular dystrophy (DMD): an in-vitro proton NMR spectroscopy study. Magnetic Resonance Imaging, 21145-153. doi:10.1016/S0730-725X(02)00646-X

Thibaud, J., Wary, C., Moullec, S., Azzabou, N., Le Guiner, C., Garcia, L., . . . Carlier, P. (2012). Quantitative evaluation of locoregional high venous pressure rAAV8-U7-ESE6-ESE8 exon-skipping therapy in the GRMD dog using NMR H-1 imaging and P-31 spectroscopy. *Neuromuscular Disorders*, 22(9-10), 859-859. doi:10.1016/j.nmd.2012.06.188

Triplett, W., Forbes, S. C., DeVos, S., Lott, D. J., Willcocks, R. J., Senesac, C., & ... Sweeney, H. L. (2013). Skeletal Muscles of Ambulant Children with Duchenne Muscular Dystrophy: Validation of Multicenter Study of Evaluation with MR Imaging and MR Spectroscopy. *Radiology*, 269(1), 198-207.

Wary, C., Naulet, T., Thibaud, J., Monnet, A., Blot, S., & Carlier, P. G. (2012). Splitting of pi and other 31P NMR anomalies of skeletal muscle metabolites in canine muscular dystrophy: 31P NMR anomalies in skeletal muscle of dystrophic dogs. *NMR in Biomedicine*, 25(10), 1160-1169. doi:10.1002/nbm.2785

Wary, C., Azzabou, N., Giraudeau, C., Le Louër, J., Montus, M., Voit, T., . . . Carlier, P. (2015). Quantitative NMRI and NMRS identify augmented disease progression after loss of ambulation in forearms of boys with duchenne muscular dystrophy. *NMR in Biomedicine*, 28(9), 1150-1162. doi:10.1002/nbm.3352

Wehling-Henricks, M., Oltmann, M., Rinaldi, C., Myung, K., & Tidball, J. (2009). Loss of positive allosteric interactions between neuronal nitric oxide synthase and phosphofructokinase contributes to defects in glycolysis and increased fatigability in muscular dystrophy. *Human Molecular Genetics*, 18(18), 3439-3451.

Willcocks, R. J., Rooney, W. D., Triplett, W. T., Forbes, S. C., Lott, D. J., Senesac, C. R., & ... Vandenborne, K. (2016). Multicenter prospective longitudinal study of magnetic resonance biomarkers in a large Duchenne muscular dystrophy cohort. *Annals of Neurology*, 79(4), 535-547. doi:10.1002/ana.24599

Vohra, R. S., Lott, D., Mathur, S., Senesac, C., Deol, J., Germain, S., & ... Vandenborne, K. (2015). Magnetic Resonance Assessment of Hypertrophic and Pseudo-Hypertrophic Changes in Lower Leg Muscles of Boys with Duchenne Muscular Dystrophy and Their Relationship to Functional Measurements. *Plos ONE*, 10(6), 1-17. doi:10.1371/journal.pone.0128915

Appendix

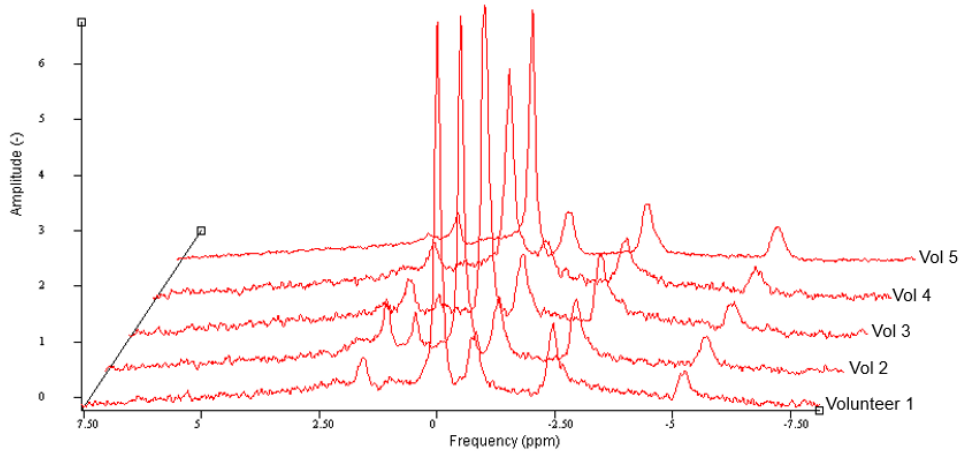

Figure 1. Presentation of the seven peaks of interest in the non-localized day 1 scan of volunteers 1-5.

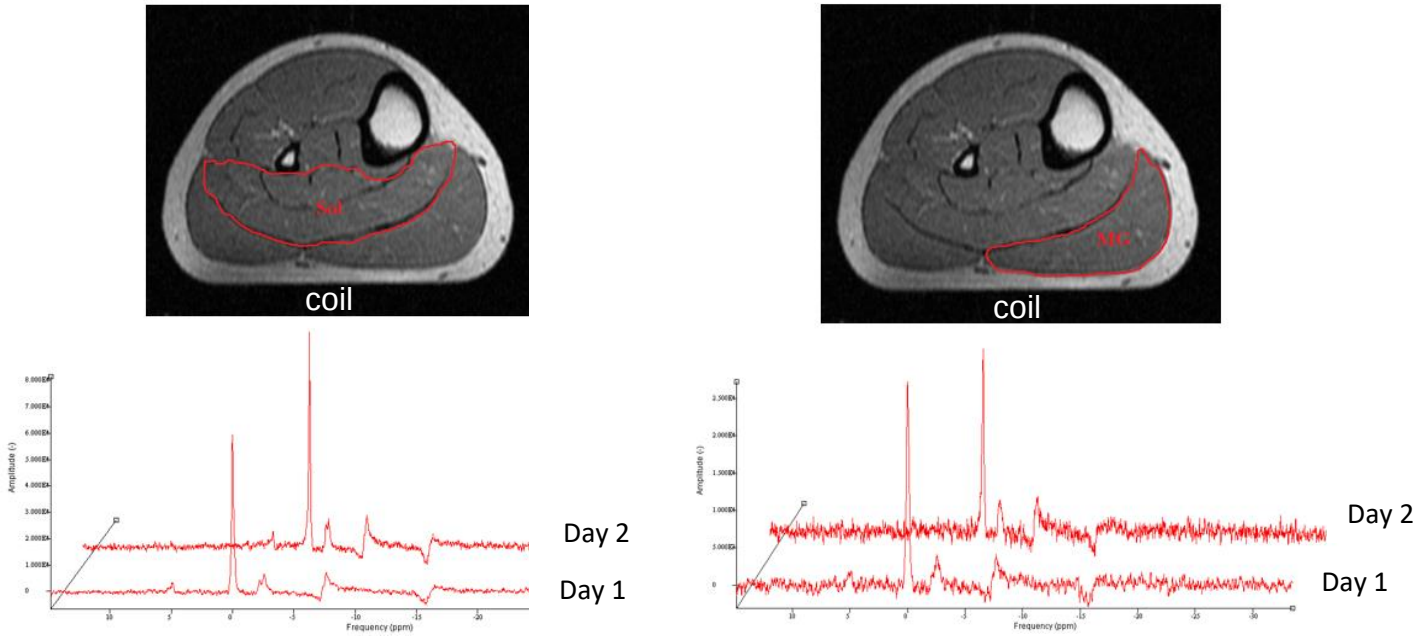

Figure 2. Multivoxel 4×4 spectra from the Sol (left) and MG (right) of volunteer 1 from both days scanned.

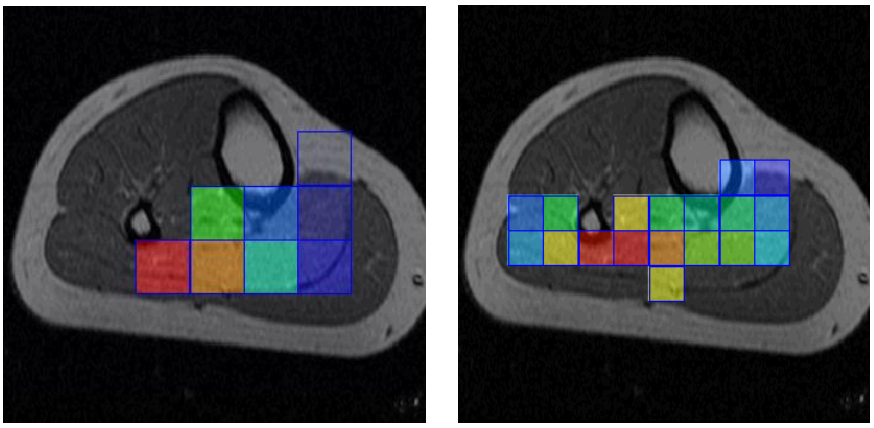

Figure 3. A comparison of 4×4 (left) and 8×8 (right) voxels selected from the Sol of volunteer 3 on the second day scanned. Voxels which had 75% of their surface area overlapping the muscle of interest were utilized for analysis.

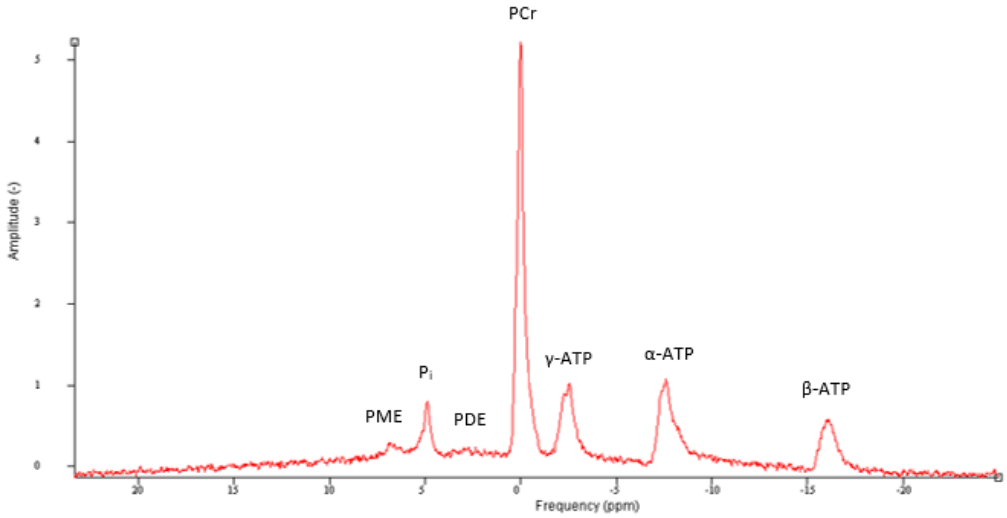

Figure 4. Non-localized spectra collected from volunteer 5 on the first day scanned.

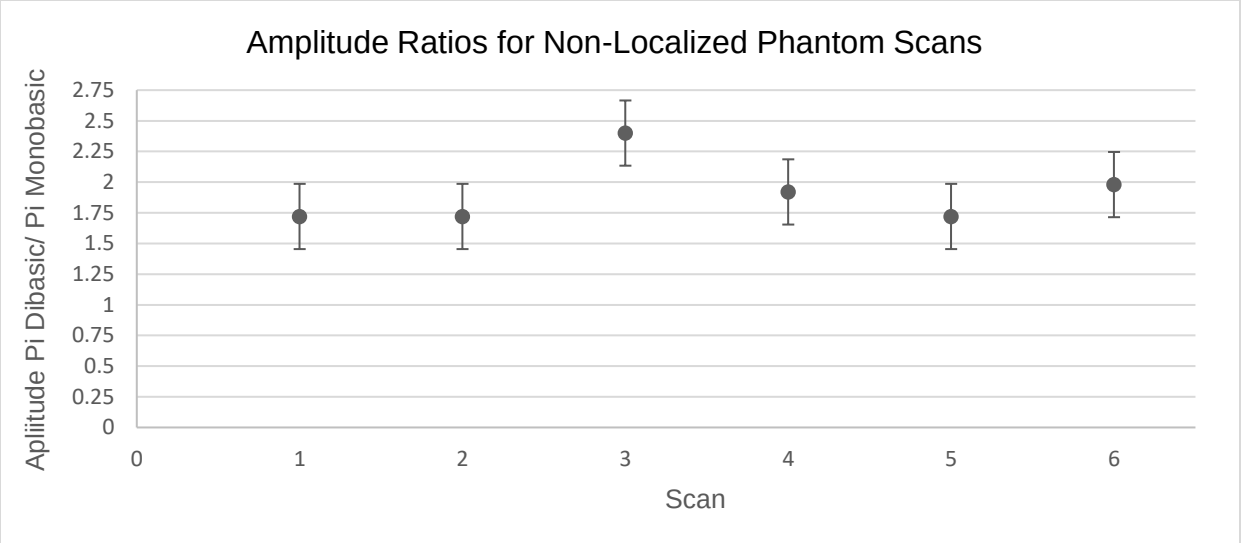

Figure 5. Amplitude ratios for non-localized phantom scans labeled with error bars representing standard deviation (scan 1: 5/18/2017, scan 2: 5/24/2017, scan 3: 7/24/2017, scan 4: 8/4/2017, scan 5: 9/29/2017, scan 6: 10/20/2017). Scan 7 was excluded from this data set due to poor shim.

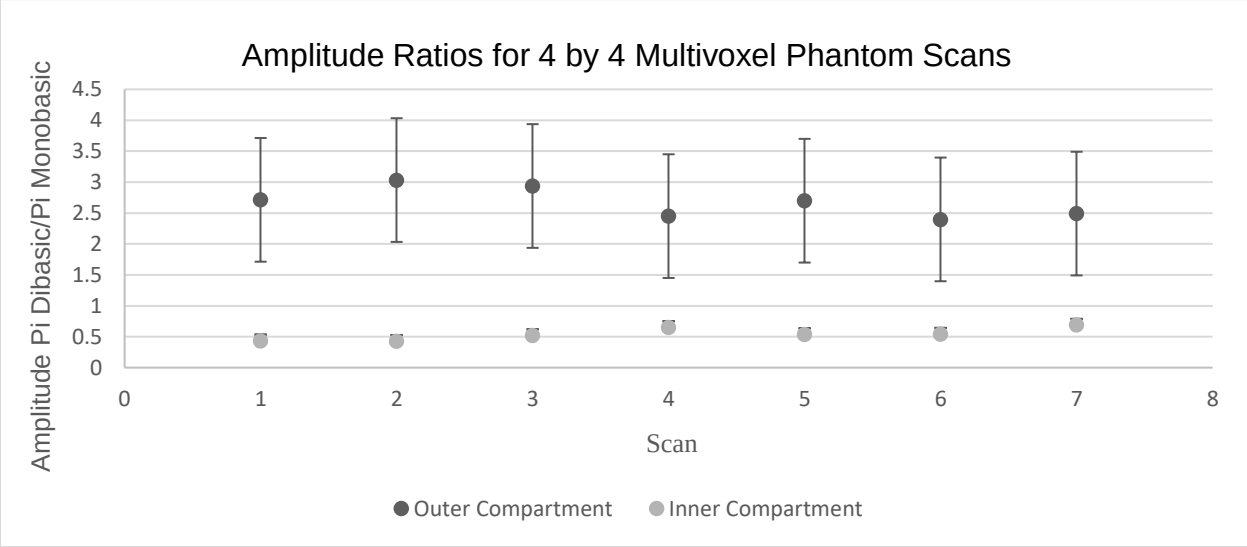

Figure 6. Amplitude ratios for spatially localized phantom scans labeled with error bars representing standard deviation (scan 1: 5/18/2017, scan 2: 5/24/2017, scan 3: 7/24/2017, scan 4: 8/4/2017, scan 5: 9/29/2017, scan 6: 10/20/2017, scan 7: 11/16/2017).

Table 1.

Averages of Day 1 and Day 2 Non-Localized CV(%) for All Subjects

	Volunteer 1	Volunteer 2	Volunteer 3	Volunteer 4	Volunteer 5	Average	St Dev
ATP/P_{tot}	12%	2.1%	6.1%	5.2%	4.5%	*5.9%	0.036
$PCr/\ _{\beta}ATP$	42%	37%	35%	6.9%	17%	28%	0.15
$PCr/\ _{\gamma}ATP$	14%	5.9%	7.2%	18%	3.7%	*9.6%	0.059
PCr/ATP	22%	9%	9.9%	13%	6.4%	12%	0.059
PCr/Ptot	10%	7%	3.8%	7.6%	1.6%	*6.1%	0.034
$PDE/\ _{\beta}ATP$	25%	11%	42%	12%	27%	23%	0.13
$PDE/\ _{\gamma}ATP$	3.7%	21%	14%	12%	14%	13%	0.063
PDE/ATP	4.7%	18%	17%	7.2%	17%	13%	0.063
PDE/Ptot	7%	20%	11%	2%	12%	10%	0.067
$Pi_{tot}/\ _{\beta}ATP$	28%	2.7%	40%	31%	29%	26%	0.14
$Pi_{tot}/\ _{\gamma}ATP$	0.62%	29%	12%	6.5%	16%	13%	0.11
Pi_{tot}/ATP	7.7%	26%	15%	12%	19%	16%	0.07
Pi_{tot}/Ptot	4%	28%	8.9%	17%	14%	14%	0.09
Pi_b/PCr	31%	41%	31%	13%	46%	32%	0.13
Pi_a/PCr	13%	34%	0.96%	29%	8.6%	17%	0.14
Pi_{tot}/PCr	14%	35%	5.1%	24%	12%	18%	0.12
Pi_b/Pi_a	18%	7.7%	30%	41%	38%	27%	0.14
Pi_b/P_{tot}	20%	35%	35%	20%	47%	31%	0.12
Pi_a/P_{tot}	2.3%	27%	4.8%	22%	10%	13%	0.11
PME/P_{tot}	7.5%	66%	17%	3.1%	19%	23%	0.25
pH	0.29%	0%	0.40%	0.6%	0.099%	*0.28%	0.0024

Note. ATP was defined as [(α-ATP+ γ-ATP+ β-ATP)/3], and P_{tot} was defined as (P_i+PCr+ α-ATP+ γ-ATP+ β-ATP).

Table 2.

Averages of Day 1 and Day 2 Multivoxel Soleus CV(%) for All Subjects

	Vol 1 (4×4)	Vol 2 (4×4)	Vol 3 (4×4)	Vol 4 (4×4)	Vol 5 (5×5)	Average	St Dev
ATP/P_{tot}	5.1%	1.8%	15%	3.4%	11%	*7.4%	0.057
$PCr/\beta ATP$	5.9%	3.4%	44%	25%	29%	21%	0.17
$PCr/\gamma ATP$	13%	2.6%	27%	6.1%	12%	12%	0.095
PCr/ATP	14%	0.33%	32%	6.7%	20%	15%	0.12
PCr/P_{tot}	8.7%	1.5%	17%	3.2%	9.2%	*8%	0.063
$PDE/\beta ATP$	33%	78%	43%	20%	---	43%	0.25
$PDE/\gamma ATP$	26%	76%	27%	0.28%	---	32%	0.32
PDE/ATP	26%	72%	31%	0.84%	---	32%	0.29
PDE/P_{tot}	31%	68%	17%	2.7%	---	30%	0.28
$P_i/\beta ATP$	33%	58%	17%	21%	49%	36%	0.17
$P_i/\gamma ATP$	26%	57%	0.12%	2.2%	34%	24%	0.24
P_i/ATP	25%	53%	5.1%	2.7%	41%	25%	0.22
Pi/P_{tot}	30%	49%	10%	0.73%	31%	24%	0.19
Pi/PCr	38%	52%	27%	4%	22%	29%	0.18
PME/P_{tot}	37%	2.6%	22%	35%	86%	36%	0.31
pH	0.30%	0.10%	0.30%	0.10%	0.30%	*0.22%	0.0011

Note. PDE data from the Sol of volunteer 5 on the first day scanned was excluded from analysis due to poor shim.

Table 3.

Averages of Day 1 and Day 2 Multivoxel Medial Gastrocnemius CV(%) for all Subjects

	Vol 1 (4×4)	Vol 2 (4×4)	Vol 3 (4×4)	Vol 4 (4×4)	Vol 5 (5×5)	Average	St Dev
ATP/P_{tot}	14%	2.1%	0.28%	23%	21%	37%	0.11
PCr/ $_{\beta}$ATP	18%	16%	19%	64%	67%	13%	0.26
PCr/ $_{\gamma}$ATP	23%	13%	0.32%	30%	0.04%	23%	0.13
PCr/ATP	24%	9.6%	5.8%	38%	37%	11%	0.15
PCr/P_{tot}	10%	7.6%	5.5%	16%	17%	64%	0.05
PDE/ $_{\beta}$ATP	68%	58%	60%	60%	75%	63%	0.072
PDE/ $_{\gamma}$ATP	72%	61%	44%	25%	110%	63%	0.34
PDE/ATP	72%	63%	49%	34%	97%	59%	0.24
PDE/P_{tot}	62%	65%	49%	11%	110%	48%	0.35
P_i/ $_{\beta}$ATP	33%	31%	29%	66%	78%	33%	0.23
P_i/ $_{\gamma}$ATP	38%	35%	47%	32%	15%	42%	0.12
P_i/ATP	39%	38%	41%	41%	50%	31%	0.05
Pi/P_{tot}	26%	39%	41%	18%	31%	25%	0.095
Pi/PCr	16%	46%	46%	2.5%	15%	57%	0.20
PME/P_{tot}	59%	2.2%	---	43%	120%	57%	0.5
pH	0.20%	1.7%	0.60%	0%	0%	*0.5%	0.0071

Note. PME data from the MG of volunteer 3 on the first day scanned was excluded from analysis due to poor shim.

Table 4.

CV and Standard Deviation of Volunteers 1, 3 & 4 Multivoxel 8×8 Scans

	Sol 8×8		MG 8×8		TA 8×8	
	CV (%)	St Dev	CV(%)	St Dev	CV(%)	St Dev
ATP/Ptot	*6.6%	0.0075	11%	0.014	18%	0.018
PCr/ βATP	26%	4.4	66%	13	96%	33
PCr/ γATP	11%	0.39	29%	0.96	20%	0.59
PCr/ATP	*8.4%	0.42	18%	0.81	23%	1.3
PCr/Ptot	*2.1%	0.012	*7.4%	0.042	*9.2%	0.054
PDE/ βATP	42%	0.54	28%	0.08	79%	0.43
PDE/ γATP	47%	0.12	73%	0.08	89%	0.14
PDE/ATP	44%	0.17	97%	0.098	130%	0.34
PDE/Ptot	36%	0.016	90%	0.011	130%	0.032
Pi/ βATP	22%	0.55	71%	1.3	105%	6.6
Pi/ γATP	26%	0.13	29%	0.095	*9.9%	0.049
Pi/ATP	23%	0.17	12%	0.05	*6.3%	0.057
Pi/Ptot	17%	0.014	*1.2%	0.00064	*8.1%	0.0079
Pi/PCr	17%	0.024	13%	0.013	12%	0.021
PME/Ptot	70%	0.025	120%	0.0082	49%	0.012
pH	*0.16%	0.012	*0.41%	0.029	*3.8%	0.27